

RLV Integrated Guidance and Control Based on Adaptive High-order Sliding Mode

Zhiyu Li¹, bailing tian¹, and Xiuyun Zhang¹

¹Tianjin University School of Electrical and Information Engineering

May 4, 2023

Abstract

In this paper, a novel integrated guidance and control algorithm based on adaptive high-order sliding mode is proposed for reusable launch vehicle (RLV) subject to unknown disturbances and actuator faults. We propose a time-varying barrier function-based adaptive control law to offset the effects of uncertainties. The remarkable feature of the developed algorithm is its ability to track the reference commands in finite time despite unknown disturbances and actuator faults, without designing the guidance law and attitude controller separately. Finally, the effectiveness of the proposed algorithm is confirmed by the simulation results.

RESEARCH ARTICLE

RLV Integrated Guidance and Control Based on Adaptive High-order Sliding Mode

Zhiyu Li | Bailing Tian | Xiuyun Zhang

School of Electrical and Information
Engineering, Tianjin University, Tianjin
300072, China

Correspondence

*Xiuyun Zhang. Email: zxy_11@tju.edu.cn

Abstract

In this paper, a novel integrated guidance and control algorithm based on adaptive high-order sliding mode is proposed for reusable launch vehicle (RLV) subject to unknown disturbances and actuator faults. We propose a time-varying barrier function-based adaptive control law to offset the effects of uncertainties. The remarkable feature of the developed algorithm is its ability to track the reference commands in finite time despite unknown disturbances and actuator faults, without designing the guidance law and attitude controller separately. Finally, the effectiveness of the proposed algorithm is confirmed by the simulation results.

KEYWORDS:

Reusable launch vehicle, Integrated guidance and control, Adaptive control, High-order sliding mode

1 | INTRODUCTION

Since RLV suffers from complex external disturbances and actuator faults, especially in the reentry phase, the design of the guidance and control (G&C) system with sufficient robustness is essential to ensure stable flight. The traditional structure of G&C consists of two parts, in which guidance subsystem and attitude control subsystem are usually designed separately. The main purpose of RLV reentry guidance is to establish a closed loop feedback relationship between guidance and trajectory, ensuring the safe transition from the initial reentry point to the target point on the premise of meeting the flight corridor, and providing feasible reference guidance commands for attitude control system.¹ Generally, two strategies are considered to create guidance commands. The first strategy stores the reentry trajectory calculated offline, and compares it with the actual flight data in advance to obtain the feedback guidance law.^{2,3,4,5} The second strategy is called predictor-corrector guidance method. It does not rely on the reference trajectory, but constantly predicts the end of the flight and adjusts the control amount according to the deviation between the prediction and the desired target.^{6,7,8,9} When the guidance commands are obtained, the design of attitude control system is necessary to track the guidance commands in the presence of unknown external disturbances. Sliding Mode Control (SMC) as a special nonlinear control is attractive in practice because of its inherent insensitivity and complete robustness against external disturbances.¹⁰ To reduce control chattering in traditional SMC, a quasi-continuous HOSMC is designed for RLV with bounded comprehensive disturbances, which could provide high accuracy in realization.¹¹ However, the upper bounds of disturbances are required in the controller design, which is not feasible in some practical applications. Thus, the issue has motivated the researchers to develop adaptive sliding mode. In the work of Tian et al,¹² an adaptive multivariable finite-time control algorithm based on super-twisting algorithm is proposed and applied in attitude control of RLV with unknown disturbances. However, the obtained adaptive gain is overestimated, which may increase the chattering associated with unmodeled dynamics¹³. To address the issue, an adaptive multivariable control algorithm is developed, utilizing a time-varying barrier function to design the adaptive control gain, which is ensured to be as small as possible but large enough to resist the disturbances.¹⁴

Although much work has been done to improve the performance of separate G&C, instability may still be caused by the spectral separation between the guidance and attitude subsystems and the subsystems are redesigned separately when the overall system performance is inadequate, which is costly, time-consuming, and satisfactory results may not be guaranteed.¹⁵ In contrast to the traditional G&C, integrated guidance and control (IGC) regards the guidance system and the control system as a single-loop system. It is able to improve the coordination and matching degree of G&C system. Moreover, it can reduce the amount of design iterations, with less cost and calculation time. Due to the potential advances, many researchers have developed methods in IGC design, such as small-gain method,¹⁶ inverse dynamic method,¹⁷ robust model predictive control (MPC) method,¹⁸ barrier Lyapunov function-based method¹⁹ and so on. Moreover, methods based on backstepping approach have been widely studied in IGC system design, since the system has strict feedback form. In²⁰, a backstepping based multiconstraints adaptive scheme is developed, in which a saturation function is employed to guarantee the prescribed performance. In the work of Zhang et al,²¹ the global finite-time stability of RLV closed-loop system is guaranteed, and the feasibility of backstepping method is verified. However, differential explosion phenomenon may occur when using backstepping approach.

SMC is also a potential candidate for IGC, and HOSMC can mitigate the problem of arbitrary degree dynamic system. In the work of Cross and Shtessel,²² a HOSMC based smooth controller within the single-loop IGC structure is presented for a missile interceptor, where the upper bounds of disturbances are required in the IGC design. Nevertheless, in RLV practical applications, disturbances with unknown upper bounds are usually present. Thus, the issue has motivated the researchers to develop adaptive HOSMC. In the work of Harmouche et al,²³ a Lyapunov based adaptive HOSMC is proposed. The presented controller gain can be adjusted in both increasing and decreasing directions rapidly. Further research were made and an adaptive controller using the barrier functions is proposed to achieve the finite-time convergence of the sliding variable without the knowledge of the upper bounds of disturbances.²⁴ In the method, an explicit bound on the control is provided. Nevertheless, a detection mechanism is required to ensure the adaptive controller coefficient switching between the linear function and barrier function, which is nontrivial in RLV practical applications.

Motivation and contribution: It can be observed that most of the existing research on RLV control designs the guidance system and attitude control system separately,^{1,14,25} which may cause spectral separation. Therefore, inspired by the work of Cross and Shtessel,²² we take the guidance and control system as a high-order system and design the controller within the single-loop integrated and control structure. As for the control theory aspect, considering the high-order input/output model with the effect of unknown efficiency loss and external disturbances, and to avoid the detection mechanism in the work of Laghrouche et al,²⁴ a novel barrier function-based adaptive high-order sliding mode control algorithm that take effect from the initial time is developed. Motivated by the above observations, the main contribution of this paper can be summarized in the following two aspects.

1) We present an adaptive high-order sliding mode control algorithm ensuring the finite-time convergence of solutions to a prescribed function from the initial time, without utilizing the knowledge of upper bounds of disturbances.

2) The developed algorithm is applied to integrated guidance and control system of RLV, and the tracking requirements of RLV are fulfilled with the developed algorithm, overcoming the effects of unknown external disturbances and control efficiency loss.

Compared with the existing results,^{1,14,25} a single-loop guidance and control structure is introduced for RLV, and it offers the opportunity to control the vehicle using a single feedback path, which makes the vehicle easier to design. Compared with the existing result,²⁴ the proposed algorithm ensures the finite-time convergence of solutions to a prescribed function from the initial time, rather than a switched vicinity of origin, such that the detection mechanism is avoided.

The structure of the remainder of this paper is organized as follows. The problem studied in this research is formulated in Section II. In Section III, the adaptive HOSMC is provided in detail and the proposed algorithm is applied to IGC system design for RLV. Some representative simulation tests are provided in Section IV. Finally, the conclusion and future work are presented in Section V.

2 | PROBLEM FORMULATION

2.1 | Integrated guidance and control Model

In this paper, the unpowered RLV system is considered, whose nominal IGC model can be described by a set of translation and rotation differential equations as²⁵

$$\begin{cases} \dot{h} = v \sin \gamma, \\ \dot{v} = -D - g \sin \gamma, \\ \dot{\gamma} = \frac{1}{v} L \cos \sigma + \left(\frac{v}{h+R_E} - \frac{g}{v} \right) \cos \gamma, \\ \dot{\alpha} = -p \cos \alpha \tan \beta + q - r \sin \alpha \tan \beta, \\ \dot{\beta} = p \sin \alpha - r \cos \alpha, \\ \dot{\sigma} = -p \cos \alpha \cos \beta - q \sin \beta - r \sin \alpha \cos \beta, \\ \dot{p} = I_{p,x} M_x + I_{p,z} M_z + I_{p,pq} pq + I_{p,qr} qr, \\ \dot{q} = I_{q,y} M_y + I_{q,p} p^2 + I_{q,r} r^2 + I_{q,pr} pr, \\ \dot{r} = I_{r,x} M_x + I_{r,z} M_z + I_{r,pq} pq + I_{r,qr} qr, \end{cases} \quad (1)$$

where h represents the flight altitude; v is velocity; γ is flight path angle; α , β , σ denote attack angle, sideslip angle and bank angle, respectively; p , q , r denote roll, pitch and yaw angular rates; g is the gravity acceleration and R_E is radius of Earth, whereas L and D are the lift and drag accelerations denoted by $L = \rho v^2 S C_L / 2m$ and $D = \rho v^2 S C_D / 2m$, where ρ is atmospheric density, S and m represent the mass and reference area of the vehicle; the aerodynamic coefficients are given by $C_L = cl_0 + cl_1 \alpha$ and $C_D = cd_0 + cd_1 \alpha + cd_2 \alpha^2$. $I_{p,x}, \dots, I_{r,qr}$ are moments inertia coefficients whose expressions are given in the Appendix.A. The control inputs are M_x roll moment, M_y pitch moment and M_z yaw moment. The main objective of the present work is to develop an IGC algorithm which makes altitude, velocity and sideslip angle track their desired values. The block diagram of IGC system of RLV in this paper is presented in Fig.1.

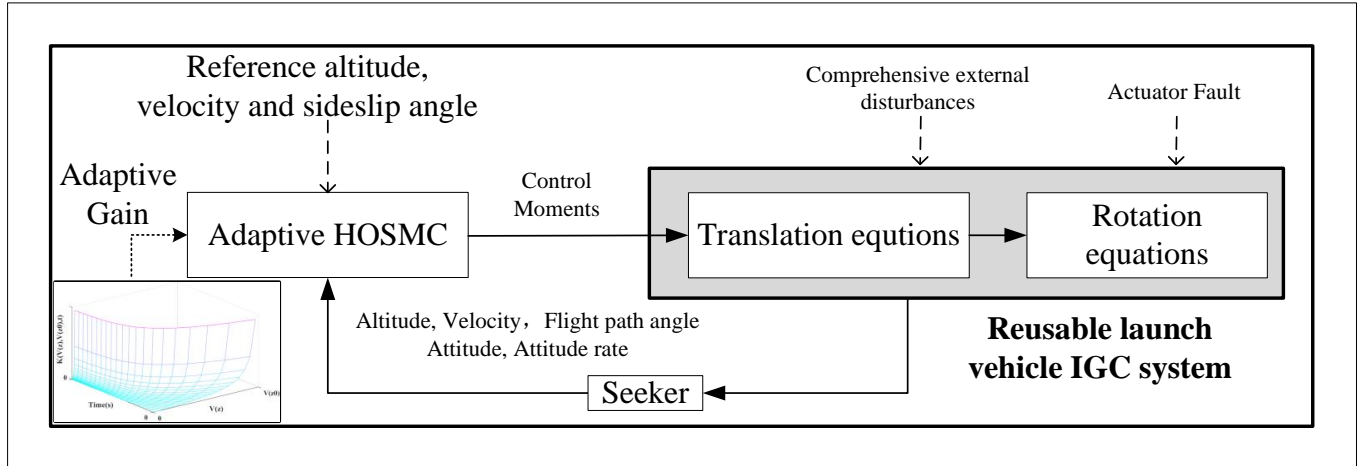


Figure 1 Integrated guidance and control architecture

2.2 | Input/Output Linearization

Considering the tracking requirements of the IGC system, the sliding surface can be established as

$$s_h = h - h_{ref}, \quad s_v = v - v_{ref}, \quad s_\beta = \beta - \beta_{ref}. \quad (2)$$

Then, to facilitate controller design, we differentiate the sliding surface such that it can be written in a form in which control moments appear explicitly. Taking the derivatives of the altitude and velocity, the following formulas are obtained

$$\begin{aligned} h^{(4)} &= \ddot{v} \sin \gamma + \ddot{\gamma} v \cos \gamma + 3\dot{v}\dot{\gamma} \cos \gamma + \dot{v} (3\ddot{\gamma} \cos \gamma - 3\dot{\gamma}^2 \sin \gamma) - v (3\ddot{\gamma} \dot{\gamma} \sin \gamma + \dot{\gamma}^3 \cos \gamma). \\ \ddot{v} &= -\ddot{D} - \ddot{g} \sin \gamma - 2\dot{g}\dot{\gamma} \cos \gamma - g\ddot{\gamma} \cos \gamma + g\dot{\gamma}^2 \sin \gamma. \end{aligned} \quad (3)$$

where the Drag and lift acceleration derivatives with respect to time can be computed as

$$\begin{aligned}\ddot{L} &= L\left(\frac{\ddot{\rho}}{\rho} + 2\frac{\dot{v}}{v} + 2\frac{\dot{v}^2}{v^2} + \frac{\dot{C}_L}{C_L} + 2\frac{\dot{\rho}C_L}{\rho C_L} + 4\frac{\dot{v}C_L}{vC_L} + 4\frac{\dot{v}\dot{\rho}}{v\rho}\right), \\ \ddot{D} &= D\left(\frac{\ddot{\rho}}{\rho} + 2\frac{\dot{v}}{v} + 2\frac{\dot{v}^2}{v^2} + \frac{\dot{C}_D}{C_D} + 2\frac{\dot{\rho}C_D}{\rho C_D} + 4\frac{\dot{v}C_D}{vC_D} + 4\frac{\dot{v}\dot{\rho}}{v\rho}\right),\end{aligned}\quad (4)$$

It is assumed that the atmospheric density ρ and the gravity acceleration g depend only on the altitude. And the time derivatives of the aerodynamic coefficients can be computed as

$$\begin{aligned}\dot{C}_L &= cl_1\dot{\alpha}, & \dot{C}_D &= 2cd_2\alpha\dot{\alpha} + cd_1\dot{\alpha}, \\ \ddot{C}_L &= cl_1\ddot{\alpha}, & \ddot{C}_D &= (2cd_2\alpha + cd_1)\ddot{\alpha} + 2cd_2\dot{\alpha}^2.\end{aligned}\quad (5)$$

By differentiating the attitude angles twice with respect to time, we have the controls appearing in \dot{p} , \dot{q} and \dot{r} ,

$$\begin{aligned}\ddot{\alpha} &= -\dot{p}\cos\alpha\tan\beta + p\left(\dot{\alpha}\sin\alpha\tan\beta - \dot{\beta}\frac{\cos\alpha}{\cos^2\beta}\right) + \dot{q} - \dot{r}\sin\alpha\tan\beta - r\left(\dot{\alpha}\cos\alpha\tan\beta + \dot{\beta}\frac{\sin\alpha}{\cos^2\beta}\right), \\ \ddot{\beta} &= \dot{p}\sin\alpha + p\dot{\alpha}\cos\alpha - \dot{r}\cos\alpha + r\dot{\alpha}\sin\alpha, \\ \ddot{\sigma} &= -\dot{p}\cos\alpha\cos\beta + p(\dot{\alpha}\sin\alpha\cos\beta + \dot{\beta}\cos\alpha\sin\beta) - \dot{q}\sin\beta - q\dot{\beta}\cos\beta - \dot{r}\sin\alpha\cos\beta - r(\dot{\alpha}\cos\alpha\cos\beta - \dot{\beta}\sin\alpha\sin\beta).\end{aligned}\quad (6)$$

With all these relationships, taking the actuator faults and external disturbances in to consideration, the entire linearized input/output model can be obtained, which has the following compact form

$$\dot{\mathbf{S}} = \mathbf{A} + \delta\mathbf{B}\mathbf{M} + \mathbf{D}.\quad (7)$$

The matrices \mathbf{S} , \mathbf{A} , \mathbf{B} , \mathbf{M} are defined as

$$\mathbf{S} = \begin{bmatrix} \ddot{s}_h \\ \ddot{s}_v \\ \ddot{s}_\beta \end{bmatrix}, \quad \mathbf{A} = \begin{bmatrix} a_h - \ddot{h}_{ref}^{(4)} \\ a_v - \ddot{v}_{ref} \\ a_\beta - \ddot{\beta}_{ref} \end{bmatrix}, \quad \mathbf{B} = \begin{bmatrix} b_{h,x} & b_{h,y} & b_{h,z} \\ b_{v,x} & b_{v,y} & b_{v,z} \\ b_{\beta,x} & b_{\beta,y} & b_{\beta,z} \end{bmatrix}, \quad \mathbf{M} = \begin{bmatrix} M_x \\ M_y \\ M_z \end{bmatrix}, \quad \mathbf{D} = \delta\mathbf{B}\mathbf{\Delta}_M + \begin{bmatrix} \Delta_h \\ \Delta_v \\ \Delta_\beta \end{bmatrix},\quad (8)$$

where the expressions for the terms $a_h, a_v, \dots, b_{\beta,z}$ in \mathbf{A} and \mathbf{B} are given explicitly in Appendix.A, whose values depend on the states which are known at every moment if all system states are measurable. $\mathbf{\Delta}_M$ denotes additive actuator fault and $\delta(t)$ denotes the efficiency loss function with $\delta_m \leq \delta(t) \leq 1$; $\Delta_h, \Delta_v, \Delta_\beta$ represent the external disturbances imposed on each channel; M_x, M_y and M_z are the control moments needed to be determined.

Assumption 1. It is assumed that all the states in model (1) are available for feedback.

Remark 1. Taking the control moments as the control input, the relative degree of (7) is $4 + 3 + 2 = 9$, equals to the order of IGC system. Thus, the nonlinear model can be linearized completely²⁶. Moreover, with the states available in model (1), the system's higher-order derivatives of states could be obtained by rigorous mathematical expressions.

In next section, we will provide the adaptive HOSMC algorithm, which can ensure system (7) convergent to the origin in finite time.

3 | ADAPTIVE HIGH-ORDER SLIDING MODE CONTROLLER

To facilitate controller design, extent the input/output IGC model (7) to a general r th-order system of

$$\begin{cases} \dot{z}_i = z_{i+1}, & i = 1, \dots, n-1, \\ \dot{z}_n = a(t) + \delta(t)u + d(t), \end{cases}\quad (9)$$

where z_1 is the output which can be replaced by s_h for $n = 4$, s_v for $n = 3$ and s_β for $n = 2$ to obtain the model (7). z_2, \dots, z_n are internal variable and u is the system input. $a(t)$ is the known term related to the system state, which is one term in matrix \mathbf{A} in (8) for the particular case. $d(t)$ is the unknown disturbance related to \mathbf{D} , and $\delta(t)$ is the efficiency loss function.

In what follows, the proposed algorithm is developed base on (9) without loss of generality. With the controller defined by $u = \tilde{u} - a(t)$, (9) can be transformed into

$$\dot{z}_n = \delta(t)\tilde{u} + \underbrace{d(t) + (1 - \delta)a(t)}_{\zeta(t)}.\quad (10)$$

Then, without loss of generality, the developed algorithm is progressed on (10). Moreover, from a practical point of view, the system states and the uncertainty are always bounded as it is derived from a finite vehicle response, so the following assumption could be made to facilitate controller design.

Assumption 2. It is assumed that the uncertain function $\zeta(t)$ is bounded with unknown upper bound and there exist constant $\bar{\zeta} > 0$ such that $|\zeta_m| \leq \bar{\zeta}$ holds.

We now present an adaptive time-varying high-order sliding mode controller for system (10), and the construction of the proposed algorithm relies on the following lemma:

Lemma 1.²⁷ Consider system (10) with $\delta \equiv 1$ and $\zeta \equiv 0$. Suppose there exists a continuous state-feedback control law $\tilde{u} = \tilde{u}_0(z)$, a positive definite C^1 function $V(z) : R^r \rightarrow R_+$, and real numbers $c > 0$ and $0 < \eta < 1$, such that the following condition is true for every trajectory z of system (10)

$$\dot{V}(z) \leq -cV(z)^\eta. \quad (11)$$

Then system (10) with the feedback $\tilde{u}_0(z)$ is globally finite time stable with respect to the origin.

Regarding our problem, an adaptive function is adopted to handle the disturbances. In the spirit of the work of Laghrouche et al²⁴, with the knowledge of the initial value of the system, the adaptive function is defined based on the following time-varying barrier function

$$K(V(z), V(z_0), t) = \frac{V(z)}{f(V(z_0), t) - V(z)}, \quad (12)$$

where $z_0 = z(0)$, and $V(z)$ is provided by Lemma 1. $f : R_+ \rightarrow R_+$ is a non-increasing C^1 function, with $\lim_{t \rightarrow +\infty} f(V(z_0), t) \geq 0$ and $f(V(z_0), 0) = \epsilon + V(z_0)$, where ϵ is tuning positive constant.

Remark 2. Note that the adaptive gain changes according to the value of $V(z)$. When $V(z)$ increases towards the boundary of $f(V(z_0), t)$, K increases accordingly, which forces the state to converge, and then K decreases till it could compensate the disturbance. Compared with the barrier function-based piecewise function in the work of Laghrouche et al²⁴, the time-varying barrier function in (12) allows $V(z)$ to stay within $f(V(z_0), t)$ from the initial instant, so the detection mechanism can be avoided.

The following theorem summarizes the main results of the developed algorithm.

Theorem 1. Considering system (10) with Assumption 1, if the feedback control law is defined by:

$$\tilde{u}(z, t) = k_1 \tilde{u}_0(z) + k_2 K \text{sign}(\tilde{u}_0(z)), \quad (13)$$

where k_1 and k_2 are positive tuning parameters, K is the time-varying adaptive function defined in (12). $\tilde{u}_0(z)$ is any state-feedback control law that satisfies Lemma 1 and obeys the following further conditions:

$$\frac{\partial V}{\partial z_n} \tilde{u}_0(z) \leq 0, \tilde{u}_0(z) = 0 \Rightarrow \frac{\partial V}{\partial z_n} = 0. \quad (14)$$

where $V(z)$ is the corresponding Lyapunov function satisfies Lemma 1. Then system (10) with the feedback $\tilde{u}(z, t)$ is globally finite time stable with respect to the origin, and function $V(z)$ will be confined in the prescribed region $f(V(z_0), t)$.

Proof 1. Consider system (10) and the control law defined in (13):

$$\begin{cases} \dot{z}_i = z_{i+1}, i = 1, \dots, n-1, \\ \dot{z}_n = \delta [k_1 \tilde{u}_0 + k_2 K \text{sign}(\tilde{u}_0)] + \zeta. \end{cases} \quad (15)$$

Considering the Lyapunov function in Lemma 1 with a new control input $\tilde{u}(z, t)$, We can obtain the following inequality for the time derivative of $V(z)$ along the system (10).

$$\begin{aligned} \dot{V} &= \sum_{i=1}^{n-1} \frac{\partial V}{\partial z_i} z_{i+1} + \frac{\partial V}{\partial z_n} (\delta [k_1 \tilde{u}_0 + k_2 K \text{sign}(\tilde{u}_0)] + \zeta) \\ &= \sum_{i=1}^{n-1} \frac{\partial V}{\partial z_i} z_{i+1} + \frac{\partial V}{\partial z_n} \tilde{u}_0 + \frac{\partial V}{\partial z_n} [(\delta k_1 - 1) \tilde{u}_0 + \delta k_2 K \text{sign}(\tilde{u}_0) + \zeta]. \end{aligned} \quad (16)$$

Notice that $\sum_{i=1}^{n-1} \frac{\partial V}{\partial z_i} z_{i+1} + \frac{\partial V}{\partial z_n} \tilde{u}_0 = \dot{V} \leq -cV(z)^\eta$ according to (11), and $(\partial V / \partial z_n) \tilde{u}_0 \leq 0$ holds according to the condition in (14). Therefore, we have

$$\dot{V} \leq -cV^\eta - \left| \frac{\partial V}{\partial z_r} \right| \left[(\delta_m k_1 - 1) |\tilde{u}_0| + \delta_m k_2 K - \bar{\zeta} \right]. \quad (17)$$

For brevity, define the following function

$$F(V(z)) = K - \underbrace{\frac{1}{\delta_m k_2} \left(\bar{\zeta} + (1 - \delta_m k_1) |\tilde{u}_0| \right)}_{\Phi}, \quad (18)$$

and taking into account the definition of K in (12), the solution of $F(V(z)) = 0$ yields a unique solution $V_*(t)$ in $(0, f(V(z_0), t))$, as $V_*(t) = (\Phi / (1 + \Phi)) f(V(z_0), t) < f(V(z_0), t)$. Arguing by contradiction, one gets that $V(z(t)) > V_*(t)$ for all non-negative time, and hence leads to $\dot{V} < -cV^\eta$. And this yields convergence to the origin in finite time, which is a contradiction. Then it can be deduced that system (10) is finite time stable with respect to the origin for all $V(z(t)) > V_*(t)$, and $V(z)$ is decreasing accordingly, which leads to $V(z(t)) < V_*(t) < f(V(z_0), t)$. In conclusion, $V(z)$ will always be confined in the prescribed region $f(V(z_0), t)$ from the initial instant. ■

In what follows, the algorithm in the work of Hong²⁸ will be utilized to develop the controller law $\tilde{u}_0(z)$. To show that, with $|x|^\lambda$ denotes $|x|^\lambda \text{sign}(x)$, the controller is defined as follows:

Let $\kappa < 0$ and l_1, \dots, l_n be positive real numbers. For $z = (z_1, \dots, z_n)$, the controller $\tilde{u}_0(z) = v_n$ can be defined as

$$v_{i+1} = -l_{i+1} \left[|z_{i+1}|^{\lambda_i} - |v_i|^{\lambda_i} \right]^{\frac{\mu_{i+1}}{\lambda_i}}, \quad i = 1, \dots, n, \quad (19)$$

where $m_i = 1 + (i - 1)\kappa$, $\lambda_0 = m_2$, $(\lambda_i + 1)m_{i+1} = \lambda_0 + 1$ and $\mu_i = m_{i+1}/m_i$. And the Lyapunov function V is defined as

$$V = \sum_{j=1}^n \int_{v_{j-1}}^{z_j} |s|^{\lambda_{j-1}} - |v_{j-1}|^{\lambda_{j-1}} ds. \quad (20)$$

With the definition of V , the conditions in (14) can be verified by

$$\frac{\partial V}{\partial z_n} v_n = -l_n \left[|z_n|^{\lambda_{n-1}} - |v_{n-1}|^{\lambda_{n-1}} \right]^{1 + \frac{\mu_n}{\lambda_{n-1}}} \leq 0, \quad (21)$$

and $v_n = 0$ if and only if $\partial V / \partial z_n = 0$.

Finally, with the development of the feedback controller in (13), the adaptive HOSMC algorithm applied to RLV system can be summarized as the following proposition.

Proposition 1. Considering IGC input/output model (7), if the control moment vector \mathbf{M} is designed by

$$\mathbf{M} = \mathbf{B}^{-1}(\mathbf{U} - \mathbf{A}), \quad (22)$$

with virtual control vector \mathbf{U} designed by

$$\mathbf{U} = \begin{bmatrix} k_1 \tilde{u}_0(s_h) + k_2 K(V(s_h), V(s_{h0}), t) \text{sign}(\tilde{u}_0(s_h)) \\ k_1 \tilde{u}_0(s_v) + k_2 K(V(s_v), V(s_{v0}), t) \text{sign}(\tilde{u}_0(s_v)) \\ k_1 \tilde{u}_0(s_\beta) + k_2 K(V(s_\beta), V(s_{\beta0}), t) \text{sign}(\tilde{u}_0(s_\beta)) \end{bmatrix}. \quad (23)$$

where the nominal controllers $\tilde{u}_0(s_h)$, $\tilde{u}_0(s_v)$, $\tilde{u}_0(s_\beta)$ and Lyapunov functions $V(s_h)$, $V(s_v)$, $V(s_\beta)$ are designed based on the algorithm in the work of Hong²⁸, whose explicitly forms are given in Appendix.B. Then the RLV system could be able to track the reference altitude $h_{ref}(t)$, velocity $v_{ref}(t)$ and sideslip angle $\beta_{ref}(t)$.

Proof of Proposition 1. Since model (7) is a special case of the general r th-order system (9) discussed in Theorem 1, the convergence of the IGC tracking system can be proved, similar to Proof 1, which is omitted here.

4 | SIMULATION RESULTS ANALYSIS

In this section, simulation experiments are provided to demonstrate the effectiveness of the developed algorithm. The RLV characteristic parameters used in this paper are based on X-33²⁹, with the aerodynamic parameters provided by $cl_0 = -0.2070$, $cl_1 = 1.6756$, $cd_0 = 0.0785$, $cd_1 = -0.3529$, $cd_2 = 2.0400$. The inertia coefficients can be obtained by substituting

$I_{xx} = 434270\text{kg} \cdot \text{m}^2$, $I_{yy} = 961220\text{kg} \cdot \text{m}^2$, $I_{zz} = 1131541\text{kg} \cdot \text{m}^2$, $I_{xz} = 17880\text{kg} \cdot \text{m}^2$ into (I.1) in Appendix.I. The sampling time is selected as 1ms.

To obtain the reference commands $h_{ref}(t)$ and $v_{ref}(t)$, trajectory optimization method in the work of Darby et al³⁰ is adopted, with the starting point set as $h_0 = 80000\text{m}$, $v_0 = 7800\text{m/s}$ and $\gamma_0 = -1^\circ$. In addition, according to the steady turn requirements, the sideslip angle is controlled to $\beta_{ref}(t) = 0$. Then for perturbed RLV system, initial longitudinal state deviations are set to $[\Delta h_0, \Delta v_0, \Delta \beta_0] = [-500\text{m}, 100\text{m/s}, 1^\circ]$, additive actuator faults are given as $[\Delta M_x, \Delta M_y, \Delta M_z] = 10^6 * [0.3 \sin(0.1t), 1 + 0.3 \cos(0.1t), 0.3 \cos(0.1t)]$ and efficiency loss function is set to $\delta = 0.9 + 0.1 \cos(0.1t)$. Finally, we make a comparison between the proposed IGC algorithm and the separate guidance and control (SGC) strategy developed in the work of Tian et al¹².

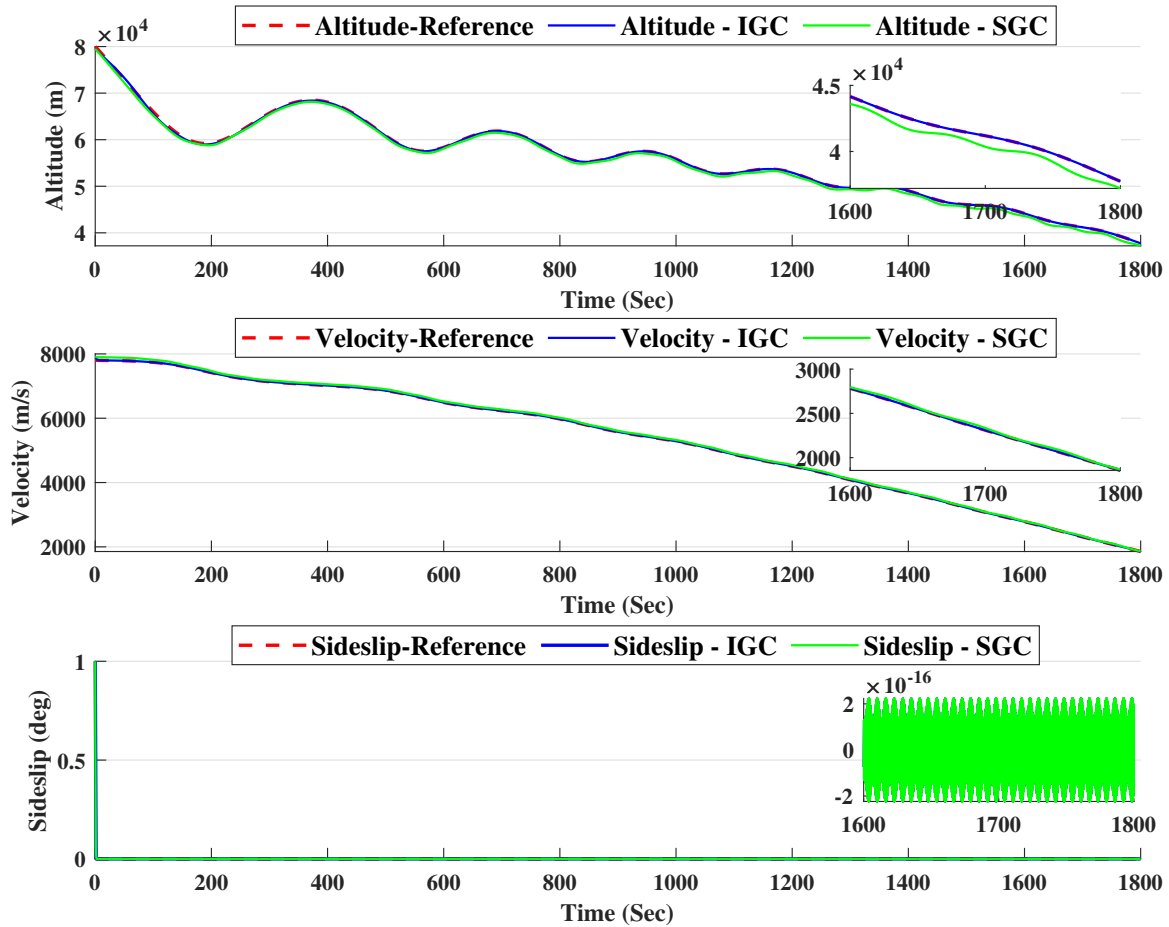


Figure 2 Curves of altitude, velocity and sideslip angle

Figs.3-4 illustrate the trajectory tracking results of RLV system. From the results, it can be observed that developed IGC algorithm can effectively drive the RLV to track the desired reference command, overcoming the effects of disturbances and actuator faults. Meanwhile, despite the perturbations in initial condition could be handled by the SGC method in the previous work¹², other uncertainties, especially actuator faults, may lead to the failure of the SGC system, as shown in Figs.3-4. Moreover, derivatives of the tracking errors of IGC system are provided in Fig.4, revealing the effective convergence performance of the developed adaptive HOSMC. The convergence time of the system is mainly related to the initial deviation and the parameters of the nominal controllers \tilde{u}_0 . Finally, the system control moments are shown in Fig.5. The above results verify the effectiveness of the developed IGC scheme based on adaptive HOSMC even in complex disturbance environment.

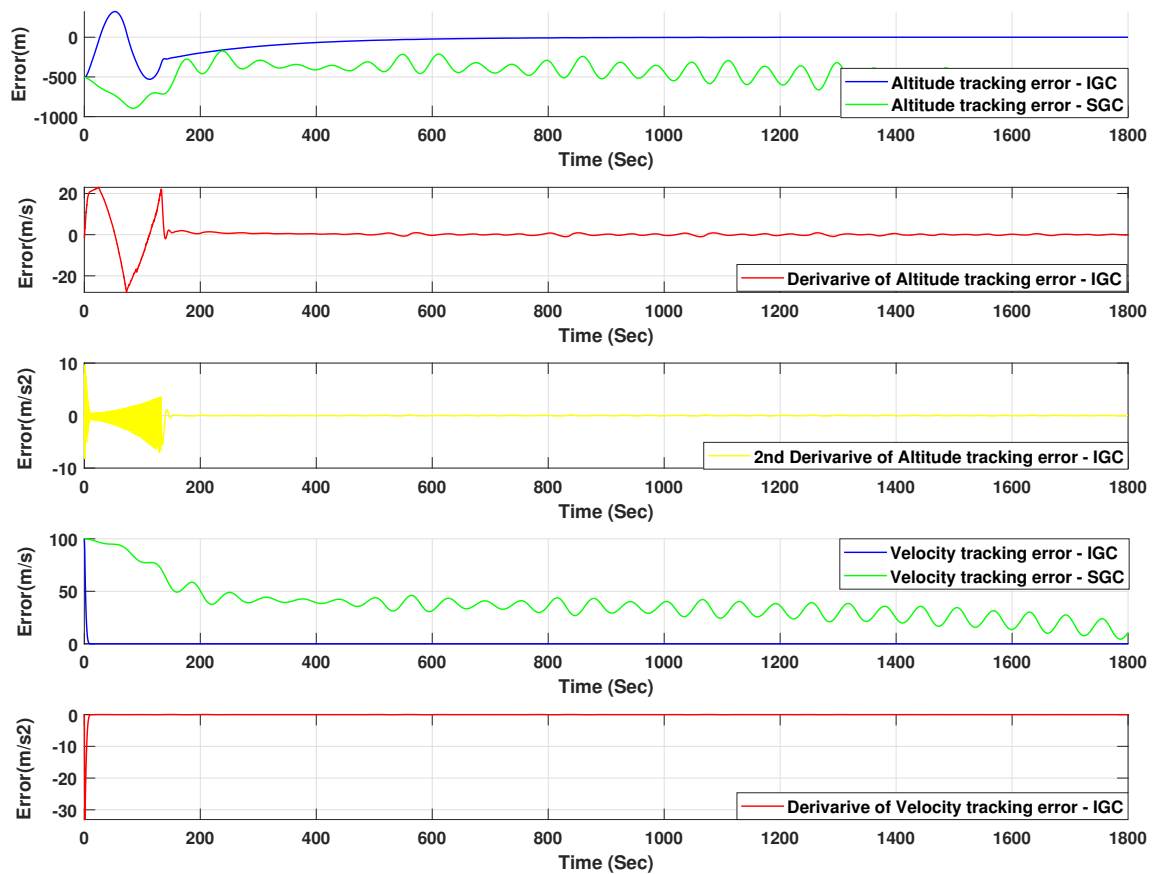


Figure 3 Curves of altitude, velocity tracking errors and their derivatives

5 | CONCLUSIONS

A novel adaptive high-order sliding mode based integrated guidance and control algorithm is developed for RLV with unknown disturbances and actuator faults. A time-varying barrier function based adaptive controller is adopted to restrict the RLV tracking error from the initial instant without utilizing the upper bounds disturbances. The developed algorithm is compared with a separate guidance and control method, and simulation results demonstrate that the proposed IGC system has better robust performance and can ensure the system state to track the reference trajectory in finite time. Future work will focus on the combination of the proposed algorithm and fixed-time high-order sliding mode control method.

6 | ACKNOWLEDGMENTS

This work was supported in part by the National Natural Science Foundation of China under Grant 62022060, 62073234, 62003236, 61773278, 61873340, 61903349.

7 | CONFLICT OF INTEREST

There is no conflict of interest.

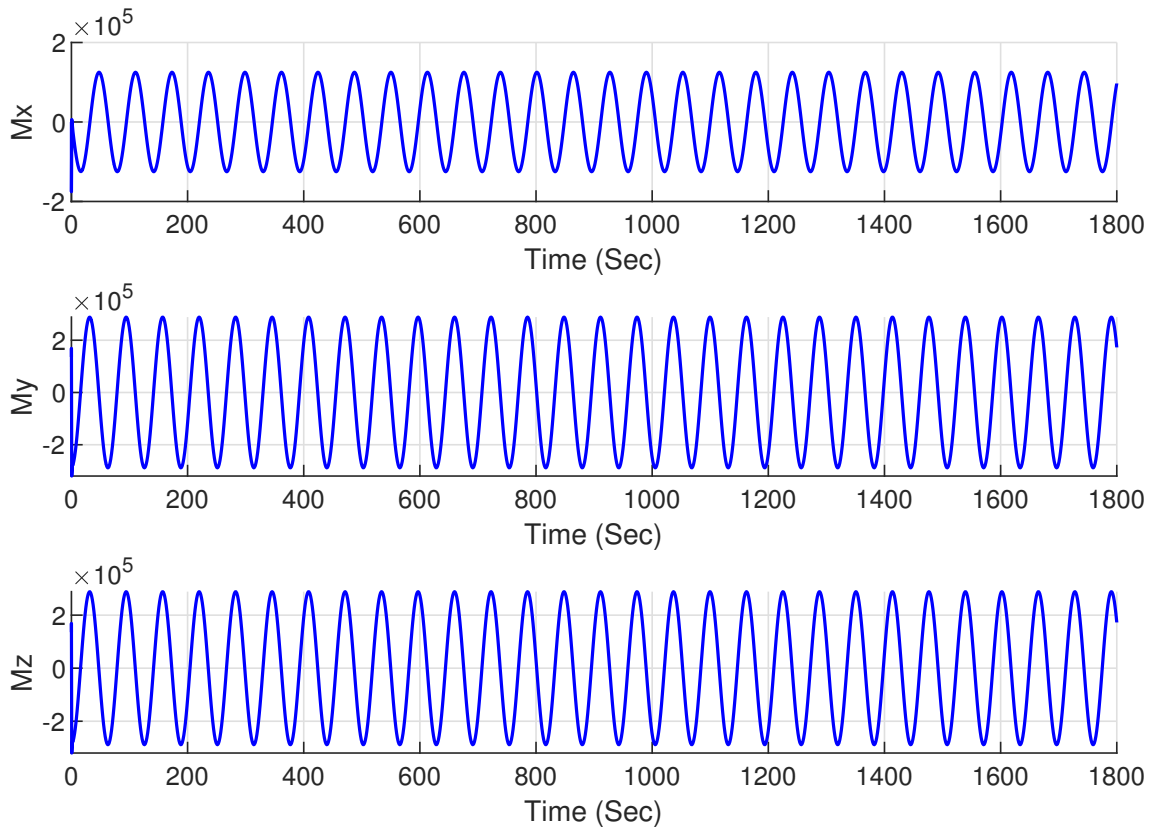


Figure 4 Curves of control moments

8 | DATA AVAILABILITY STATEMENT

The data that support the findings of this study are available from the corresponding author upon reasonable request.



APPENDIX

A RLV MOMENT INERTIAL AND INPUT/OUTPUT TERMS

The moment inertia coefficients in (1) are expressed as

$$\begin{aligned}
 I_{p,x} &= \frac{I_{zz}}{I_{xx}I_{zz} - I_{xz}^2}, I_{p,z} = I_{r,x} = \frac{I_{xz}}{I_{xx}I_{zz} - I_{xz}^2}, \\
 I_{p,pq} &= \frac{(I_{xx} - I_{yy} + I_{zz}) I_{xz}}{I_{xx}I_{zz} - I_{xz}^2}, I_{p,qr} = \frac{(I_{yy} - I_{zz}) I_{zz} - I_{xz}^2}{I_{xx}I_{zz} - I_{xz}^2}, \\
 I_{q,y} &= \frac{1}{I_{yy}}, I_{q,p} = -\frac{I_{xz}}{I_{yy}}, I_{q,r} = \frac{I_{xz}}{I_{yy}}, I_{q,pr} = \frac{I_{zz} - I_{xx}}{I_{yy}}, \\
 I_{r,z} &= \frac{I_{xx}}{I_{xx}I_{zz} - I_{xz}^2}, \\
 I_{r,pq} &= \frac{(I_{xx} - I_{yy}) I_{xx} + I_{xz}^2}{I_{xx}I_{zz} - I_{xz}^2}, I_{r,qr} = \frac{(I_{yy} - I_{xx} - I_{zz}) I_{xz}}{I_{xx}I_{zz} - I_{xz}^2}
 \end{aligned} \tag{I.1}$$

where I_{ij} ($i = x, y, z; j = x, y, z$) denotes moments inertia.

The terms $a_h, \dots, b_{\beta,z}$ in (7) can be denoted as follows:

$$a_h = a_v \sin \gamma + a_\gamma v \cos \gamma + 3\ddot{v}\dot{\gamma} \cos \gamma + \dot{v} (3\ddot{\gamma} - 3\dot{\gamma}^2 \sin \gamma) + v (-3\ddot{\gamma}\dot{\gamma} \sin \gamma - \dot{\gamma}^3 \cos \gamma) \tag{I.2}$$

$$b_{h,x} = b_{v,x} \sin \gamma + b_{\gamma,x} v \cos \gamma \tag{I.3}$$

$$b_{h,y} = b_{v,y} \sin \gamma + b_{\gamma,y} v \cos \gamma \tag{I.4}$$

$$b_{h,z} = b_{v,z} \sin \gamma + b_{\gamma,z} v \cos \gamma \tag{I.5}$$

$$\begin{aligned}
 a_v &= -a_D - \ddot{g} \sin \gamma - 2\dot{g}\dot{\gamma} \cos \gamma - g\ddot{\gamma} \cos \gamma + g\dot{\gamma}^2 \sin \gamma - D \left(\frac{\ddot{\rho}}{\rho} + 2\frac{\ddot{v}}{v} + 2\frac{\dot{v}^2}{v^2} + \frac{2cd_2\dot{\alpha}^2}{C_D} + 2\frac{\dot{\rho}\dot{C}_D}{\rho C_D} + 4\frac{\dot{v}\dot{C}_D}{v C_D} + 4\frac{\dot{v}\dot{\rho}}{v\rho} \right) \\
 &+ \frac{D(2cd_2\alpha + cd_1)p}{C_D} \left(\dot{\alpha} \sin \alpha \tan \beta - \dot{\beta} \frac{\cos \alpha}{\cos^2 \beta} \right) - \frac{D(2cd_2\alpha + cd_1)r}{C_D} \left(\dot{\alpha} \cos \alpha \tan \beta + \dot{\beta} \frac{\sin \alpha}{\cos^2 \beta} \right)
 \end{aligned} \tag{I.6}$$

$$b_{v,x} = \frac{D(2cd_2\alpha + cd_1)}{C_D} \{ I_{p,x} \cos \alpha \tan \beta + I_{r,x} \sin \alpha \tan \beta \} \tag{I.7}$$

$$b_{v,y} = -\frac{D(2cd_2\alpha + cd_1)}{C_D} I_{q,y} \tag{I.8}$$

$$b_{v,z} = \frac{D(2cd_2\alpha + cd_1)}{C_D} \{ I_{p,z} \cos \alpha \tan \beta + I_{r,z} \sin \alpha \tan \beta \} \tag{I.9}$$

$$\begin{aligned}
 a_\gamma &= \hat{a}_\gamma + \frac{\cos \sigma}{v} \left\{ L \left(\frac{\ddot{\rho}}{\rho} + 2\frac{\ddot{v}}{v} + 2\frac{\dot{v}^2}{v^2} + 2\frac{\dot{\rho}\dot{C}_L}{\rho C_L} + 4\frac{\dot{v}\dot{C}_L}{v C_L} + 4\frac{\dot{v}\dot{\rho}}{v\rho} \right) + a_L + \frac{Lcl_1 p}{C_L} \left(\dot{\alpha} \sin \alpha \tan \beta - \dot{\beta} \frac{\cos \alpha}{\cos^2 \beta} \right) \right. \\
 &- \frac{Lcl_1 r}{C_L} \left(\dot{\alpha} \cos \alpha \tan \beta + \dot{\beta} \frac{\sin \alpha}{\cos^2 \beta} \right) \left. \right\} - \frac{L \sin \sigma}{v} \left\{ p (\dot{\alpha} \sin \alpha \cos \beta - \dot{\beta} \cos \alpha \sin \beta) - r (\dot{\alpha} \cos \alpha \cos \beta - \dot{\beta} \sin \alpha \sin \beta) \right. \\
 &- q \dot{\beta} \cos \beta - (I_{p,pq} p q + I_{p,qr} q r) \cos \alpha \cos \beta - (I_{r,pq} p q + I_{r,qr} q r) \sin \alpha \cos \beta - (I_{q,p} p^2 + I_{q,r} r^2 + I_{q,pr} p r) \sin \beta \left. \right\}
 \end{aligned} \tag{I.10}$$

$$\begin{aligned} \hat{a}_\gamma = & -\frac{2\dot{L}\dot{\sigma}\sin\sigma + L\dot{\sigma}^2\cos\sigma}{v} + \frac{2L\dot{\sigma}\dot{v}\sin\sigma - 2\dot{L}\dot{v}\cos\sigma - L\ddot{v}\cos\sigma}{v^2} + \frac{2L\dot{v}^2\cos\sigma}{v^3} \\ & + \left(\frac{\dot{v}}{h+R_E} - \frac{2v\dot{h} + v\ddot{h}}{(h+R_E)^2} + \frac{2v\dot{h}^2}{(h+R_E)^3} \right) \cos\gamma - \left(\frac{\ddot{g}}{v} - \frac{2\dot{g}\dot{v} + g\ddot{v}}{v^2} + \frac{2g\dot{v}^2}{v^3} \right) \cos\gamma \end{aligned} \quad (\text{I.11})$$

$$\begin{aligned} & - 2 \left(\frac{\dot{v}}{h+R_E} - \frac{v\dot{h}}{(h+R_E)^2} - \frac{\dot{g}}{v} + \frac{g\dot{v}}{v^2} \right) \dot{\gamma} \sin\gamma - \left(\frac{v}{h+R_E} - \frac{g}{v} \right) (\ddot{\gamma} \sin\gamma + \dot{\gamma}^2 \cos\gamma). \\ b_{\gamma,x} = & -\frac{Lcl_1 \cos\sigma}{vC_L} \{ I_{p,x} \cos\alpha \tan\beta + I_{r,x} \sin\alpha \tan\beta \} + \frac{L \sin\sigma}{v} \{ I_{p,x} \cos\alpha \cos\beta + I_{r,x} \sin\alpha \cos\beta \} \end{aligned} \quad (\text{I.12})$$

$$b_{\gamma,y} = \left\{ \frac{Lcl_1 \cos\sigma}{vC_L} + \frac{L \sin\sigma}{v} \sin\beta \right\} I_{q,y} \quad (\text{I.13})$$

$$b_{\gamma,z} = -\frac{Lcl_1 \cos\sigma}{vC_L} \{ I_{p,z} \cos\alpha \tan\beta + I_{r,z} \sin\alpha \tan\beta \} + \frac{L \sin\sigma}{v} \{ I_{p,z} \cos\alpha \cos\beta + I_{r,z} \sin\alpha \cos\beta \} \quad (\text{I.14})$$

$$a_\beta = p\dot{\alpha} \cos\alpha + r\dot{\alpha} \sin\alpha + pq (I_{p,pq} \sin\alpha - I_{r,pq} \cos\alpha) + qr (I_{p,qr} \sin\alpha - I_{r,qr} \cos\alpha) \quad (\text{I.15})$$

$$b_{\beta,x} = I_{p,x} \sin\alpha - I_{r,x} \cos\alpha \quad (\text{I.16})$$

$$b_{\beta,y} = 0 \quad (\text{I.17})$$

$$b_{\beta,z} = I_{p,z} \sin\alpha - I_{r,z} \cos\alpha \quad (\text{I.18})$$

$$a_D = -\frac{D(2cd_2\alpha + cd_1)}{C_D} \left\{ (I_{p,pq}pq + I_{p,qr}qr) \cos\alpha \tan\beta + (I_{r,pq}qp + I_{r,qr}qr) \sin\alpha \tan\beta - (I_{q,r}r^2 + I_{q,pr}pr + I_{q,p}p^2) \right\} \quad (\text{I.19})$$

$$a_L = \frac{LC_D cl_1}{DC_L(2cd_2\alpha + cd_1)} a_D \quad (\text{I.20})$$

B CONTROLLERS AND LYAPUNOV FUNCTIONS DESIGN

In our simulation, the parameters are tuned to be: $\kappa = -1/4, l_1 = 1, l_2 = 2, l_3 = 5, l_4 = 7$. The constants λ_i are $\lambda_0 = 3/4, \lambda_1 = 4/3, \lambda_2 = 5/2, \lambda_3 = 6$. Then we get $\mu_1 = 4/3, \mu_2 = 2/3, \mu_3 = 1/2, \mu_4 = 0$. According to Hong²⁸, the controllers $\tilde{u}_0(s_h), \tilde{u}_0(s_v), \tilde{u}_0(s_\beta)$ in (23) are designed by

$$\begin{cases} v_{h_1} = -l_1 [s_h]^{\mu_1} \\ v_{h_2} = -l_2 [[s_h]^{\lambda_1} - [v_{h_1}]^{\lambda_1}]^{\frac{\mu_2}{\lambda_1}} \\ v_{h_3} = -l_3 [[s_h]^{\lambda_2} - [v_{h_2}]^{\lambda_2}]^{\frac{\mu_3}{\lambda_2}} \\ \tilde{u}_0(s_h) = v_{h_4} = -l_4 [[s_h]^{\lambda_3} - [v_{h_3}]^{\lambda_3}]^{\frac{\mu_4}{\lambda_3}}, \end{cases} \quad (\text{II.1})$$

$$\begin{cases} v_{v_1} = -l_1 [s_v]^{\mu_1} \\ v_{v_2} = -l_2 [[s_v]^{\lambda_1} - [v_{v_1}]^{\lambda_1}]^{\frac{\mu_2}{\lambda_1}} \\ \tilde{u}_0(s_v) = v_{v_3} = -l_3 [[s_v]^{\lambda_2} - [v_{v_2}]^{\lambda_2}]^{\frac{\mu_3}{\lambda_2}} \end{cases} \quad (\text{II.2})$$

$$\begin{cases} v_{\beta_1} = -l_1 [s_\beta]^{\mu_1} \\ \tilde{u}_0(s_\beta) = v_{\beta_2} = -l_2 [[s_\beta]^{\lambda_1} - [v_{\beta_1}]^{\lambda_1}]^{\frac{\mu_2}{\lambda_1}} \end{cases} \quad (\text{II.3})$$

And the Lyapunov functions $V(s_h), V(s_v), V(s_\beta)$ are defined as follows

$$\begin{cases} V_{h_1} = \frac{1}{1+\lambda_0} |s_h|^{1+\lambda_0} \\ V_{h_2} = \frac{1}{1+\lambda_1} \left(|\dot{s}_h|^{1+\lambda_1} + \lambda_1 |v_{h_1}|^{1+\lambda_1} \right) - \dot{s}_h [v_{h_1}]^{\lambda_1} + V_{h_1} \\ V_{h_3} = \frac{1}{1+\lambda_2} \left(|\ddot{s}_h|^{1+\lambda_2} + \lambda_2 |v_{h_2}|^{1+\lambda_2} \right) - \ddot{s}_h [v_{h_2}]^{\lambda_2} + V_{h_2} \\ V(s_h) = V_{h_4} = \frac{\left(|\overset{\dots}{s}_h|^{1+\lambda_3+\lambda_3} |v_{h_3}|^{1+\lambda_3} \right)}{1+\lambda_3} - \overset{\dots}{s}_h [v_{h_3}]^{\lambda_3} + V_{h_3} \end{cases} \quad (\text{II.4})$$

$$\begin{cases} V_{v_1} = \frac{1}{1+\lambda_0} |s_v|^{1+\lambda_0} \\ V_{v_2} = \frac{1}{1+\lambda_1} \left(|\dot{s}_v|^{1+\lambda_1} + \lambda_1 |v_{v_1}|^{1+\lambda_1} \right) - \dot{s}_v [v_{v_1}]^{\lambda_1} + V_{v_1} \\ V(s_v) = V_{v_3} = \frac{\left(|\ddot{s}_v|^{1+\lambda_2+\lambda_2} |v_{v_2}|^{1+\lambda_2} \right)}{1+\lambda_2} - \ddot{s}_v [v_{v_2}]^{\lambda_2} + V_{v_2} \end{cases} \quad (\text{II.5})$$

$$\begin{cases} V_{\beta_1} = \frac{1}{1+\lambda_0} |s_\beta|^{1+\lambda_0} \\ V(s_\beta) = V_{\beta_2} = \frac{\left(|\dot{s}_\beta|^{1+\lambda_1+\lambda_1} |v_{\beta_1}|^{1+\lambda_1} \right)}{1+\lambda_1} - \dot{s}_\beta [v_{\beta_1}]^{\lambda_1} + V_{\beta_1} \end{cases} \quad (\text{II.6})$$

with $V(s_{h0}), V(s_{v0}), V(s_{\beta0})$ being their initial values.

References

1. Webb KD, Lu P. *Entry guidance by onboard trajectory planning and tracking*: 0279; 2016.
2. Harpold J, Graves Jr C. Shuttle entry guidance. *American Astronautical Society* 1978.
3. Dukeman G. *Profile-following entry guidance using linear quadratic regulator theory*: 4457; 2002.
4. Tian B, Zong Q. Optimal guidance for reentry vehicles based on indirect Legendre pseudospectral method. *Acta Astronautica* 2011; 68(7-8): 1176–1184.
5. An H, Wu Q, Wang C, Cao X. Scramjet operation guaranteed longitudinal control of air-breathing hypersonic vehicles. *IEEE/ASME Transactions on Mechatronics* 2020; 25(6): 2587–2598.
6. Lu P. Predictor-corrector entry guidance for low-lifting vehicles. *Journal of Guidance, Control, and Dynamics* 2008; 31(4): 1067–1075.
7. Lu P, Brunner CW, Stachowiak SJ, Mendeck GF, Tigges MA, Cerimele CJ. Verification of a fully numerical entry guidance algorithm. *Journal of Guidance, Control, and Dynamics* 2017; 40(2): 230–247.
8. Cheng L, Jiang F, Wang Z, Li J. Multiconstrained Real-Time Entry Guidance Using Deep Neural Networks. *IEEE Transactions on Aerospace and Electronic Systems* 2020; 57(1): 325–340.
9. Zhe L, Xinsan L, Lixin W, Qiang S. Multiconstrained Gliding Guidance Based on Optimal and Reinforcement Learning Method. *Mathematical Problems in Engineering* 2021; 2021.
10. Y.Shtessel, C.Edwards, L.Fridman, A.Levant. Sliding mode control and observation. *Springer New York* 2014.
11. B.L.Tian, Q.Zong, J.Wang, F.Wang. Quasi-continuous High-order Sliding Mode Controller Design for Reusable Launch Vehicles in Reentry Phase. *Aerospace Science and Technology* 2013; 28(1): 198–207.
12. Tian B, Yin L, Wang H. Finite-time reentry attitude control based on adaptive multivariable disturbance compensation. *IEEE Transactions on Industrial Electronics* 2015; 62(9): 5889–5898.

13. Y.Shtessel , M.Taleb , F.Plestan . A novel adaptive-gain supertwisting sliding mode controller: Methodology and application. *Automatica* 2012; 48(5): 759–769.
14. Tian B, Li Z, Zhang X, Zong Q. Adaptive prescribed performance attitude control for RLV with mismatched disturbance. *Aerospace Science and Technology* 2021; 117: 106918.
15. Cross MA, Shtessel YB. *Single-Loop Integrated Guidance and Control Using High-Order Sliding-Mode Control*: 433–462; Springer . 2020.
16. Yan H, Tan S, He Y. A small-gain method for integrated guidance and control in terminal phase of reentry. *Acta Astronautica* 2017; 132: 282–292.
17. Lee H, Wei C, Cui N, Chang X. *Integrated guidance and control for reusable launch vehicles with actuator failures*: 2407; 2017.
18. Shamaghdari S, Nikraves S, Haeri M. Integrated guidance and control of elastic flight vehicle based on robust MPC. *International Journal of Robust and Nonlinear Control* 2015; 25(15): 2608–2630.
19. Liu W, Wei Y, Duan G. Barrier Lyapunov function-based integrated guidance and control with input saturation and state constraints. *Aerospace Science and Technology* 2018; 84(JAN.): 845-855.
20. Zhang D, Ma P, Wang S, Chao T. Multi-constraints adaptive finite-time integrated guidance and control design. *Aerospace Science and Technology* 2020; 107: 106334.
21. Zhenyu C, Jianguo G, Bin Z, Zongyi G, Xiaodong L. Finite-time integrated guidance and control system for hypersonic vehicles. *Transactions of the Institute of Measurement and Control* 2021; 43(4): 842–853.
22. Cross M, Shtessel YB. *Integrated guidance navigation and control using high-order sliding mode control for a missile interceptor*: 1121; 2018.
23. Harmouche M, Laghrouche S, Chitour Y. *Robust and adaptive higher order sliding mode controllers*: 6436–6441; 2012.
24. Laghrouche S, Harmouche M, Chitour Y, Obeid H, Fridman LM. Barrier function-based adaptive higher order sliding mode controllers. *Automatica* 2021; 123: 109355.
25. Tian B, Fan W, Su R, Zong Q. Real-time trajectory and attitude coordination control for reusable launch vehicle in reentry phase. *IEEE Transactions on Industrial Electronics* 2014; 62(3): 1639–1650.
26. Wang Q, Stengel RF. Robust nonlinear control of a hypersonic aircraft. *Journal of guidance, control, and dynamics* 2000; 23(4): 577–585.
27. Bhat SP, Bernstein DS. Finite-time stability of continuous autonomous systems. *SIAM Journal on Control and Optimization* 2000; 38(3): 751–766.
28. Hong Y. Finite-time stabilization and stabilizability of a class of controllable systems. *Systems & control letters* 2002; 46(4): 231–236.
29. Lu P. Entry guidance and trajectory control for reusable launch vehicle. *Journal of Guidance, Control, and Dynamics* 1997; 20(1): 143–149.
30. Darby CL, Hager WW, Rao AV. An hp-adaptive pseudospectral method for solving optimal control problems. *Optimal Control Applications and Methods* 2011; 32(4): 476–502.